On the 'Permanent' Component of NBTI

T. Grasser*, Th. Aichinger†, H. Reisinger•, J. Franco°, P.-J. Wagner*, M. Nelhiebel‡,
C. Ortolland°, and B. Kaczer°

* Christian Doppler Laboratory for TCAD at the Institute for Microelectronics, TU Wien, Austria
† KAI, Villach, Austria • Infineon, Munich, Germany ° IMEC, Leuven, Belgium ‡ Infineon Technologies, Villach, Austria

***Abstract*— A number of recent publications explain NBTI to be due to a recoverable and a more permanent component. While a lot of information has been gathered on the recoverable component, the permanent component has been somewhat elusive. We demonstrate that oxide defects commonly linked to the recoverable component also form an important contribution to the permanent component of NBTI. As such, they can contribute to both the threshold voltage shift as well as the charge pumping current. Under favorable conditions, the permanent component can show recovery rates comparable to that of the recoverable component.**

I. Introduction

Recent research indicates that two components dominantly contribute to the negative bias temperature instability (NBTI) [1–6]: while one component dominates the recovery (R) the other one has been suspected to be more or less permanent (P). It has been recently shown that the degradation can be annealed at higher temperatures [6, 7], implying that P is recoverable as well, albeit at larger timescales compared to R. The most important aspect about P is that it might determine the lifetime [6]. Unfortunately, the extraction of P is challenging as it is normally overshadowed by R. As such, our understanding of P is somewhat vague, also regarding its constituents, be it interface and/or oxide defects [3, 6], or fixed positive charges [6]. We show that considerable precautions have to be taken for accurate extraction of P, as it suffers from similar issues as typically related to the extraction of R, such as measurement *delay*, measurement *duration*, as well as stress/recovery *artifacts introduced by the measurement procedure* itself. Contrary to the work of Huard [6], who links P to interface states and an equal amount of fixed positive charge, *our analysis demonstrates that a significant fraction of P is due to switching oxide traps*, which contribute to both the threshold voltage shift ΔV_{th} and to the frequency dependent fraction of the charge pumping current.

II. Erroneous Extraction of the Permanent Component

The most straight-forward approach for the extraction of P would be to wait until the recovery of ΔV_{th} has leveled at a plateau, thus directly exposing P, see for instance Fig. 1. However, the fundamental problem here is the large timescales involved in the recovery of R, as even a short stress of $t_{\mathrm{s}} = 1\,\mu$s can lead to recovery transients of up to 1 ks, not to mention the recovery of P itself. On the other hand, P is created at a slower rate than R, making it difficult to locate plateaus within reasonable measurement times (< 1 week). As a consequence, plateaus in the recovery are rarely reported in literature [6]. (The plateau reported in [8] was not reproducible.)

Using different test technologies, from thick SiO_2 to SiON and high-κ gate stacks, we begin our analysis by highlighting some mistakes related to the extraction of P in Fig. 2:

M1: The recovery of ΔV_{th} has to be plotted on a relative logarithmic scale following the end of stress, otherwise a spurious plateau appears. Such 'plateaus' are commonly found in literature but are completely irrelevant and simply a consequence of the inadequate presentation of the data.

M2: Temperature switches to a lower temperature temporarily freeze recovery, resulting in a spurious plateau [9]. While the example temperature switch from 80 °C to 40 °C given in Fig. 2 may appear pathological, a typical real-world case appears to be given in [6]: The recovery of the devices was monitored at a high temperature on a probe-station for a day. Then, they were removed and stored at room temperature to be re-measured after some weeks. The plateaus obtained from this method are thus arbitrary.

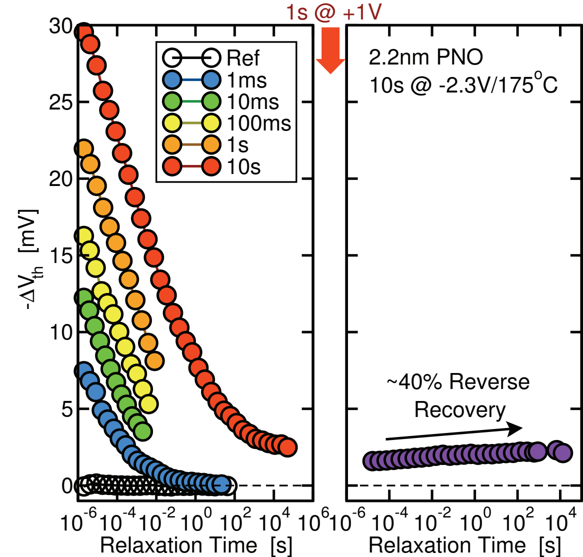

Fig. 1. Typical plateau observed under medium stress conditions. After the plateau has been reached, a positive bias was applied for a short time. For $P \sim \Delta N_{\mathrm{it}}$, one would expect ΔV_{th} to rapidly follow bias changes (within a 1 ms). In fact, a pronounced reverse recovery is observed with time constants as large as 10 ks, indicating that ΔN_{ot} can contribute to P.

M3: Application of a short positive bias partially removes oxide charges, temporarily accelerating recovery. Back at the original recovery voltage, these defects have already been annealed, resulting in a spurious plateau until the original recovery continues.

M4: In order to minimize the recovery, short stress times and low stress voltages can be chosen. This leads to relatively weak stresses and relatively short recovery times. However, particularly in thin oxides, the difference between stress and recovery voltage can be small, leading to notable degradation at the recovery voltage, interfering with the actual recovery. As a consequence, spurious plateaus can appear.

M5: Similarly to M4, charge pumping (CP) measurements can lead to degradation of ΔI_{CP} when the charge pumping amplitude is chosen too large. Balancing the recovery of ΔI_{CP}, this can lead to spurious plateaus as well, just like M4. M5 already highlights an important issue [10]: ΔI_{CP} is not constant, even within conventional measurement windows, contradicting claims [1, 6] that ΔI_{CP} is nearly constant and equal to P. In particular, the resemblance between the recovery of ΔV_{th} in M4 and ΔI_{CP} in M5 is indeed striking.

 978-1-4244-8523-9/10/$26.00 ©2010 IEEE

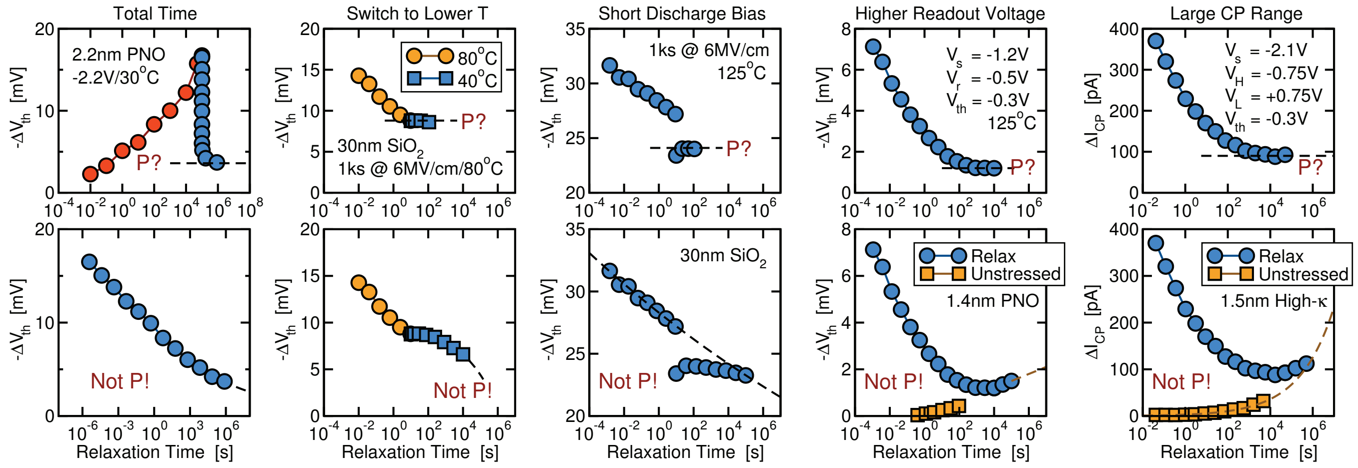

Fig. 2. Potential mistakes that have been encountered while trying to locate plateaus in $\Delta V_{\rm th}$ recovery traces. The top figures show apparent plateaus, which have nothing to do with permanent degradation. The reasons for the occurrence of these plateaus are illustrated in the bottom figures. From left to right: **(M1)** The recovery of $\Delta V_{\rm th}$ is plotted as a function of the total time, rather than the recovery time $t_{\rm r}$. Even if the recovery perfectly follows $\log(t_{\rm r})$, a spurious plateau will appear if the data is plotted this way, which has nothing whatsoever to do with P. Similar considerations relate to plotting the data on a linear scale, where the spurious plateau depends solely on the measurement time. **(M2)** Due to the large recovery time required, the device is only kept at stress temperature for a short amount of time [6] and, to ease measurement, recovery is continued at a lower temperature. This, however, is pointless, as a switch to a lower temperature freezes the recovery [9], which results in a spurious plateau. **(M3)** In order to remove R, which is due to trapped holes in the oxide [6, 11–13], a positive bias could be applied [14]. However, since the trap sites are switching traps, this has basically the same effect as a temperature switch, because such a bias switch only removes a few decades from the recovery trace, which continues after that. **(M4)** Relaxation gate voltages only slightly larger than the threshold voltage can already lead to degradation, in this example $V_{\rm relax} = -0.5\,{\rm V}$, with $V_{\rm th} = -0.3V$. As a result, degradation overlaps with the 'normal' recovery, resulting in a spurious plateau for a certain amount of time. The signature of this plateau is that it disappears when either stress or relaxation voltages are changed. **(M5)** If the charge pumping amplitude is chosen too large, for this $1.5\,{\rm nm}$ high-k device for example from $\pm 0.75\,{\rm V}$, degradation is observed during the CP measurement, again resulting in a spurious plateau as in (M4). Note the strong relaxation of $\Delta I_{\rm CP}$, which is *anything but constant*.

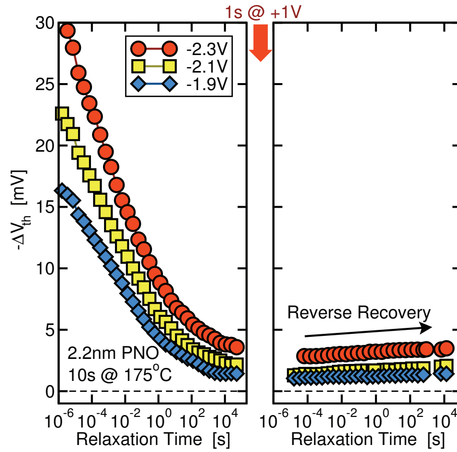

Fig. 3. Plateaus in the recovery of $\Delta V_{\rm th}$ for three different stress voltages. After short application of a positive bias pulse, again considerable reverse recovery is observed which indicates a significant contribution of slow switching oxide traps to the plateau.

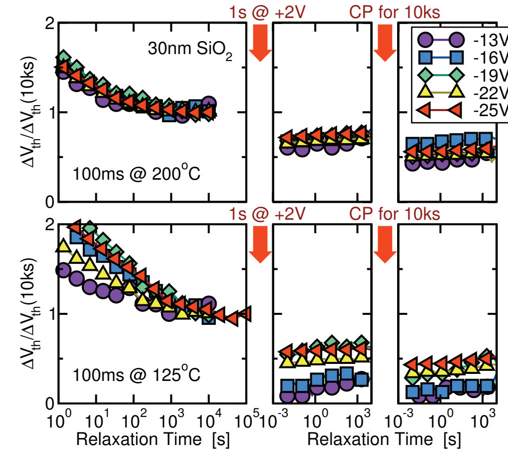

Fig. 4. The same effect as in Fig. 1 is observed on thick SiO_2 devices. The reverse recovery time constants are either somewhat larger or the application of positive bias anneals a fraction of the oxide defects, this being more pronounced at lower T. Continuous CP for $10\,{\rm ks}$ removes a further fraction, cf. Fig. 8.

III. Extraction-Attempts of the Permanent Component

We proceed by analyzing $\Delta V_{\rm th}$ recovery traces recorded after carefully selecting stress/recovery voltages, stress/recovery times, and temperature. A typical plateau at the end of the recovery is shown in Fig. 1. According to Huard [6], this plateau is due to semi-permanent interface states $\Delta N_{\rm it}$ and fixed oxide charges. Interface states are fast and can quickly follow changes in the bias ($< 1\,{\rm ms}$). Thus, a change of the interfacial Fermi-level would result in a change of the charge stored in these interface states, $\Delta Q_{\rm it}(E_{\rm F})$, according to their density-of-states. Such a change would occur rapidly, since interface states are very fast. In particular, after a temporary bias change, the same $\Delta V_{\rm th}$ would be expected back at the original bias. This is clearly not the case. In fact, $\Delta V_{\rm th}$ only slowly goes back to its original value, an apparent degradation during the recovery phase [14]. This *reverse recovery* thus indicates that a significant part of P is due to slow oxide defects, $\Delta N_{\rm ot}$, such as those observed previously [11, 13, 15]. Fig. 3 shows the bias dependence of these plateaus. Fig. 4 demonstrates this procedure on thick SiO_2 devices: application of a positive bias after having reached the plateau reduces $\Delta V_{\rm th}$ by about 40%, part of which is restored in the reverse recovery phase.

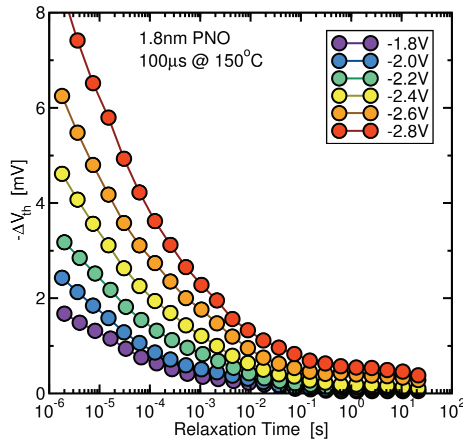

Fig. 5. Plateaus are occasionally also observed after ultra-short stress times, shown for a $1.8\,\mathrm{nm}$ PNO device. The plateau is not permanent and strongly depends on the stress bias. Particularly after such weak stresses, it is important that ΔV_{th} at the readout voltage is stable in order to avoid mistake M4 of Fig. 2.

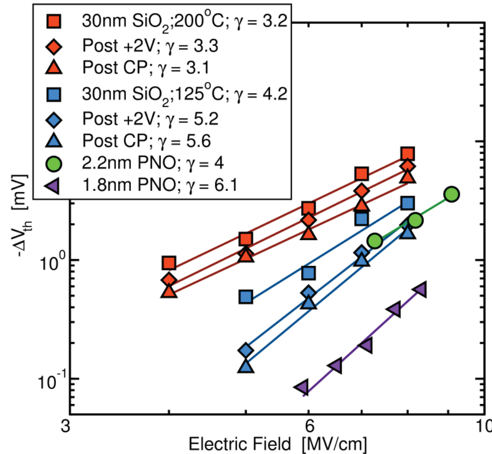

Fig. 6. The field dependence of the 'permanent' part. For the $1.8\,\mathrm{nm}$ PNO device from Fig. 5 we take $P \sim \Delta V_{\mathrm{th}}(t_{\mathrm{r}} = 1\,\mathrm{s})$, for the ones of Figs. 3 and 4 $P \sim \Delta V_{\mathrm{th}}(t_{\mathrm{r}} = 10\,\mathrm{ks})$ was chosen. In addition, for the thick $\mathrm{SiO_2}$ devices, the last value at the end of the second and third relaxation cycle are shown (10 ks after the bias switch and 10 ks after the 10 ks CP measurement). In any case, P can be fit by a power-law $\sim E_{\mathrm{ox}}^{\gamma}$.

For lifetime back-extrapolation, the bias dependence of P is crucial. Huard [6] observed $P \sim E_{\mathrm{ox}}^{\gamma}$ with a technology-independent $\gamma = 4$, without giving details on the extraction scheme for P. Fig. 5 shows plateaus appearing after a $t_{\mathrm{s}} = 100\,\mu\mathrm{s}$ stress. The E_{ox} dependence of these detected plateaus is shown in Fig. 6. Contrary to the single exponent 4 given by Huard, a wider range is observed, with values smaller and larger than 4. In contrast, the bias dependence of the plateaus in the thick $\mathrm{SiO_2}$ devices (Fig. 4) shows exponents around 3.2 at $200\,^{\circ}\mathrm{C}$ and in the range 4.2—5.6 at $125\,^{\circ}\mathrm{C}$. The latter is insofar interesting as the initial plateau has $\gamma = 4.2$, which increases to 5.2 after application of $+2\,\mathrm{V}$ for $1\,\mathrm{s}$, and even to 5.6 after continuous CP measurements for 10 ks. This again demonstrates that P, by what ever means it is extracted, is not really permanent.

IV. Correlation with Charge-Pumping Data

It has been occasionally suggested [6, 17] that P is correlated to the CP current, ΔI_{CP}. In that context, ΔI_{CP} has been interpreted as being proportional to the number of interface states. Particularly at lower frequencies it has been observed, however, that ΔI_{CP} also

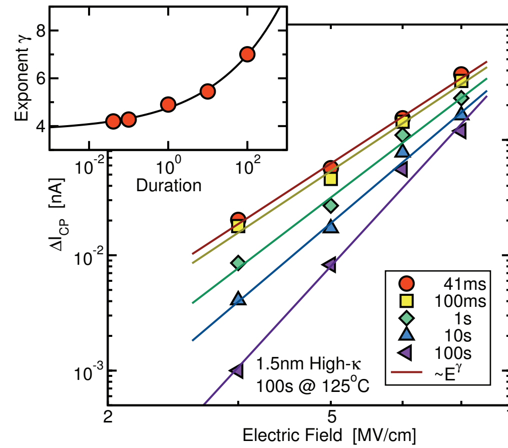

Fig. 7. The permanent component has been suggested to correlate with the change in the charge pumping current, $P \sim \Delta I_{\mathrm{CP}}$. Just like in ΔV_{th} measurements, the CP current is very sensitive to the measurement time in all our investigated technologies. This has a profound impact on the extracted bias dependence of P. Only for short CP measurements an E_{ox}^{4} dependence as in [6] is obtained.

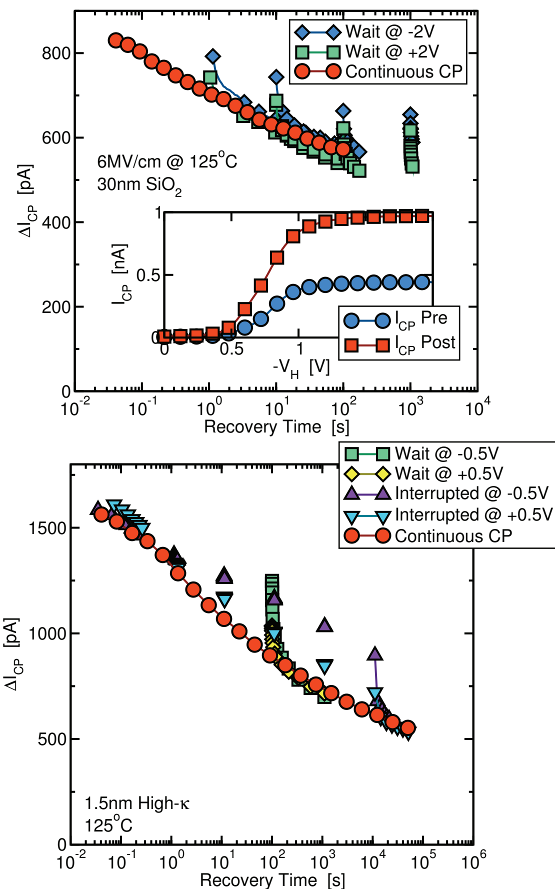

Fig. 8. Recovery of the CP current at a frequency of $1\,\mathrm{MHz}$. Contrary to other observations [6], the CP current is never constant in any of our technologies, consistent with [10]. Most importantly, continuous CP accelerates recovery. When the beginning of the CP measurement is delayed for variable amounts of time, with V_{G} being either the CP high- or low-level, rapid recovery is observed at the beginning of the delayed continuous CP measurement. Application of the CP high- and low-levels during the wait phase proves that it is not the voltage but rather the charge pumping itself that causes the rapid recovery. **Top**: For a thick $30\,\mathrm{nm}$ $\mathrm{SiO_2}$ device. **Bottom**: For a $1.5\,\mathrm{nm}$ high-κ gate stack device. The same effect is observed in both dramatically different technologies.

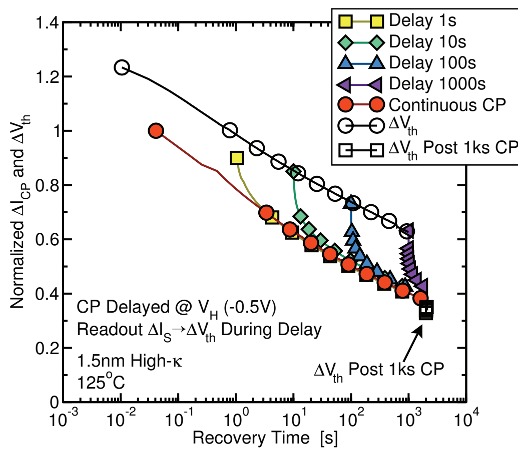

Fig. 9. Extension of the experiment in Fig. 8: the change in the linear source current ΔI_S at the CP high-level V_H is read during the wait phase and converted to ΔV_{th} following [16]. This clearly demonstrates that the onset of the accelerated CP recovery follows the recovery of ΔV_{th}. CP induced accelerated recovery in ΔI_{CP} is paralleled by a recovery in ΔV_{th} by the same fraction.

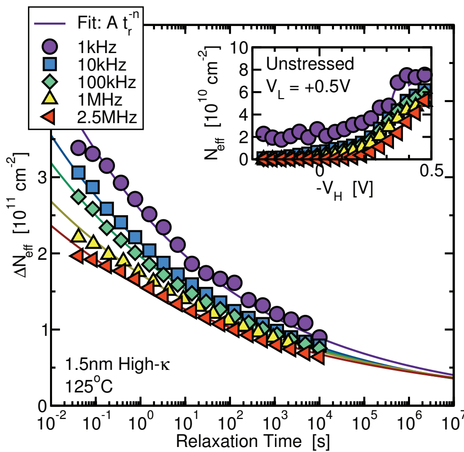

Fig. 10. Frequency dependence of the CP recovery. With lower frequency, a larger amount of oxide defects contributes to ΔN_{eff}. With increasing CP time, however, the oxide defects are 'pumped-away', giving a frequency independent ΔN_{eff} as expected from a pure ΔN_{it} contribution.

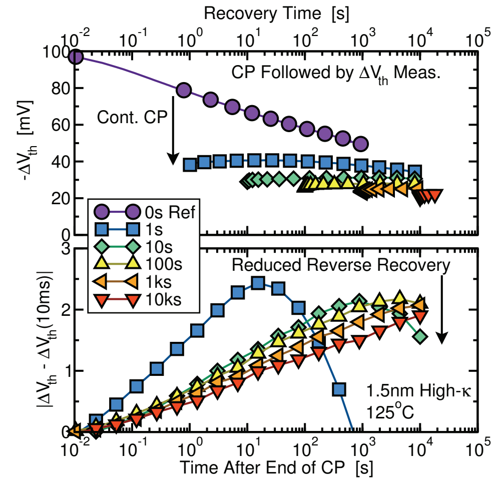

Fig. 11. Impact of continuous CP measurements with variable duration on ΔV_{th}. A considerable recovery in ΔV_{th} is observed. Also, with increasing CP duration, the reverse recovery is reduced, indicating that CP anneals slow oxide defects, ΔN_{ot}.

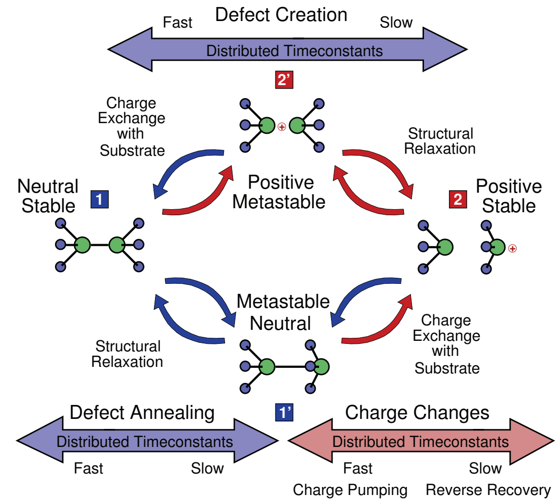

Fig. 12. The switching oxide trap model developed recently [13] is consistent with the experimentally observed behavior. Created defects can be switching traps and exchange charge with the substrate ($1' \leftrightarrow 2$), some of them faster, contributing to ΔI_{CP} in a frequency-dependent manner, some of them very slow, thus causing reverse recovery or transient RTN [13], thereby contributing to ΔV_{th} only (if in state 2).

contains considerable contributions from oxide traps [18]. This issue has been commonly neglected in the context of NBTI [19].

The bias dependence of ΔI_{CP} as a function of the measurement time is given in Fig. 7. While for fast CP experiments ($41\,\mathrm{ms}$) we obtain $\gamma = 4$, we observe a strong dependence of the extracted exponent on the duration of the CP measurement, quite similar to what is known from ΔV_{th} measurements [20], with the exponent increasing with the CP duration. This is because ΔI_{CP} shows similar recovery rates as ΔV_{th} which is contrary to Huard's work, but consistent with the observation of Rangan *et al.* [10].

Remarkably, recovery is accelerated by the CP measurement, see Fig. 8. However, in contrast to ΔV_{th} recovery, which is sensitive to bias alone [3, 20], ΔI_{CP} recovery is *accelerated by the pulsing event itself*. This accelerated recovery could be due to the large number of recombination events happening in a CP measurement, where each event releases an energy of the order of the bandgap. With 10^6 cycles per second, this accumulates to an enormous amount of energy which has to be dissipated via phonons. In due course, reactions near the defect site can be dramatically enhanced, a phenomenon known as *recombination enhanced defect reaction (REDR)* [21, 22]. Fig. 9 shows that ΔI_{CP} at the beginning of delayed CP measurements follows the recovery of ΔV_{th}. Also, the amount of recovery induced by the CP measurement is mirrored in the recovery of ΔV_{th}. This data strongly suggests that both ΔV_{th} and ΔI_{CP} are at least partially related to the same microscopic defect, namely switching oxide traps [13, 23–25]. This is confirmed by the frequency dependence of the ΔI_{CP} recovery shown in Fig. 10 which disappears after long CP times, indicating that it is oxide defects which can be 'pumped-away'. Confirmation that defects visible in ΔV_{th} react to CP measurements is given in Fig. 11: following a CP cycle, ΔV_{th} shows slow oxide defects reaching their equilibrium occupancy after long times. The reason why these switching traps can contribute to both ΔV_{th} and ΔI_{CP} is given in Fig. 12: once created, these defects can be either positive (state 2) or neutral (state $1'$), depending on the Fermi-level, the former contributing to ΔV_{th}. Transitions to state $1'$ show a wide distribution in time constants [13], with fast transitions contributing to ΔI_{CP} and slow ones responsible for the reverse recovery effect.

V. Special Case: Hydrogen-Rich Wafer

The log-like recovery of ΔI_{CP} is clearly incompatible with the recovery predicted by the reaction-diffusion (RD) model [26], $(1+\sqrt{t_{\mathrm{s}}/t_{\mathrm{r}}})^{-1}$, not depending on anything [27]. A peculiar exception has been observed on a hydrogen-rich 30 nm $\mathrm{SiO_2}$ split-wafer. Measuring ΔI_{CP} only once per decade results in $\Delta I_{\mathrm{CP}} \sim$ const. By contrast, a continuous CP measurement produces recovery traces which bear a striking resemblance to the RD prediction, particularly for $t_{\mathrm{s}} = 10$ ks, see Fig. 13. After different stress times, however, the measured recovery is practically independent of the stress-time, and does not scale universally over $t_{\mathrm{s}}/t_{\mathrm{r}}$. Still, under continuous CP conditions, recovery seems to be a diffusion-limited process in this particular wafer. An intriguing feature is that after longer stress times the devices continue to degrade after the end of stress. This is consistent with the idea that hydrogen is released during stress which then depassivates interface states and creates oxide defects [28, 29]. Otherwise, degradation after termination of the stress would not be possible. We remark that this is the standard model of irradiation damage [30].

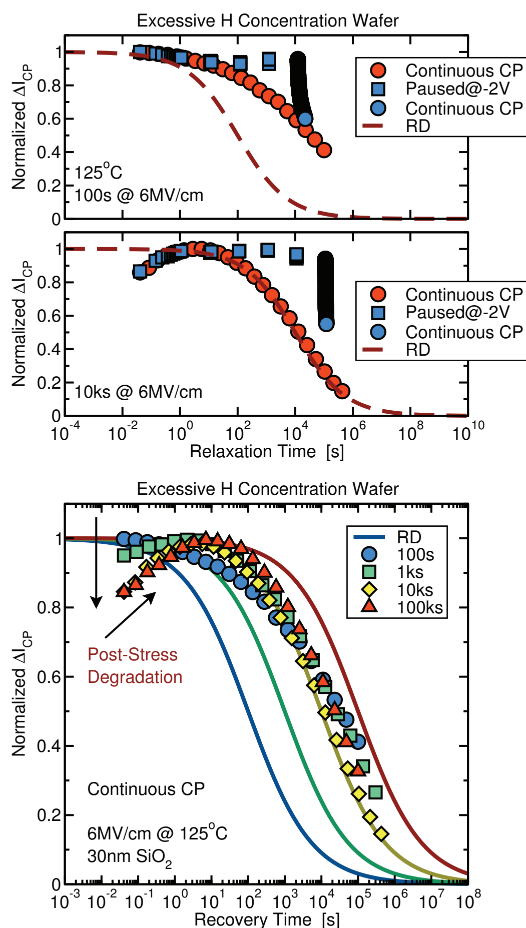

Fig. 13. **Top**: In an extremely H-rich wafer, recovery in ΔI_{CP} is basically absent provided only occasional CP measurements are made. A diffusion-limited recovery behavior seems to dominate for continuous CP measurements. **Bottom**: The recovery rate appears to be roughly independent of the stress time, meaning that the hydrogen profile is only weakly disturbed during stress. With increasing stress, though, the initial degradation during the recovery phase can last for up to 10 s and amount to 20%. This is a degradation of ΔI_{CP} which was found in this hydrogen-rich wafer only and must not be confused with the reverse recovery visible in ΔV_{th} only, cf. Fig. 11.

VI. Conclusions

We have demonstrated that the plateaus occasionally observed in carefully tuned stress/recovery experiments consist of contributions from interface states as well as slower donor-like switching oxide traps. These plateaus are not permanent and normally not too well developed. In particular, they can be annealed by applying short positive bias pulses or more effectively by continuous CP measurements. Particularly the latter provides an efficient means for annealing NBTI degradation, likely due to a recombination enhanced defect reaction mechanism. Under normal recovery conditions, the recovery of ΔV_{th} determines the starting level of ΔI_{CP}, which starts recovering quickly once CP measurements are performed. The latter demonstrates that oxide defects contribute to both ΔV_{th} and ΔI_{CP}. While the recovery rate of P is smaller than that of R, considering P as permanent will lead to serious errors, even within conventional measurement windows.

Acknowledgment

This work has received funding from the EC's FP7 grant agreement n°216436 (ATHENIS) and from the ENIAC MODERN project n°820379.

References

[1] V. Huard, M. Denais, and C. Parthasarathy, "NBTI Degradation: From Physical Mechanisms to Modelling," *Microelectronics Reliability*, vol. 46, no. 1, pp. 1–23, 2006.

[2] T. Grasser, B. Kaczer, P. Hehenberger, W. Goes, R. O'Connor, H. Reisinger, W. Gustin, and C. Schlünder, "Simultaneous Extraction of Recoverable and Permanent Components Contributing to Bias-Temperature Instability," in *Proc. Intl.Electron Devices Meeting (IEDM)*, 2007, pp. 801–804.

[3] T. Grasser, B. Kaczer, W. Goes, T. Aichinger, P. Hehenberger, and M. Nelhiebel, "A Two-Stage Model for Negative Bias Temperature Instability," in *Proc. Intl.Rel.Phys.Symp. (IRPS)*, 2009, pp. 33–44.

[4] T. Grasser and B. Kaczer, "Evidence that Two Tightly Coupled Mechanism are Responsible for Negative Bias Temperature Instability in Oxynitride MOSFETs," *IEEE Trans.Electron Devices*, vol. 56, no. 5, pp. 1056–1062, 2009.

[5] T. Aichinger, M. Nelhiebel, and T. Grasser, "A Combined Study of p and n Channel MOS Devices to Investigate the Energetic Distribution of Oxide Traps after NBTI," *IEEE Trans.Electron Devices*, vol. 56, no. 12, pp. 3018–3026, 2009.

[6] V. Huard, "Two Independent Components Modeling for Negative Bias Temperature Instability," in *Proc. Intl.Rel.Phys.Symp. (IRPS)*, 2010, pp. 33–42.

[7] C. Benard, G. Math, P. Fornara, J. Ogier, and D. Goguenheim, "Influence of Various Process Steps on the Reliability of PMOSFETs Submitted to Negative Bias Temperature Instabilities," *Microelectronics Reliability*, vol. 49, pp. 1008–1012, 2009.

[8] H. Reisinger, O. Blank, W. Heinrigs, W. Gustin, and C. Schlünder, "A Comparison of Very Fast to Very Slow Components in Degradation and Recovery Due to NBTI and Bulk Hole Trapping to Existing Physical Models," *IEEE Trans.Dev.Mat.Rel.*, vol. 7, no. 1, pp. 119–129, 2007.

[9] T. Aichinger, M. Nelhiebel, and T. Grasser, "Unambiguous Identification of the NBTI Recovery Mechanism using Ultra-Fast Temperature Changes," in *Proc. Intl.Rel.Phys.Symp. (IRPS)*, 2009, pp. 2–7.

[10] S. Rangan, N. Mielke, and E. Yeh, "Universal Recovery Behavior of Negative Bias Temperature Instability," in *Proc. Intl.Electron Devices Meeting (IEDM)*, 2003, pp. 341–344.

[11] H. Reisinger, T. Grasser, W. Gustin, and C. Schlünder, "The Statistical Analysis of Individual Defects Constituting NBTI and its Implications for Modeling DC- and AC-Stress," in *Proc. Intl.Rel.Phys.Symp. (IRPS)*, 2010, pp. 7–15.

[12] B. Kaczer, T. Grasser, P. Roussel, J. Franco, R. Degraeve, L. Ragnarsson, E. Simoen, G. Groeseneken, and H. Reisinger, "Origin of NBTI Variability in Deeply Scaled PFETs," in *Proc. Intl.Rel.Phys.Symp. (IRPS)*, 2010, pp. 26–32.

[13] T. Grasser, H. Reisinger, P.-J. Wagner, W. Goes, F. Schanovsky, and B. Kaczer, "The Time Dependent Defect Spectroscopy (TDDS) Technique for the Bias Temperature Instability," in *Proc. Intl.Rel.Phys.Symp. (IRPS)*, 2010, pp. 16–25.

[14] T. Grasser, B. Kaczer, and W. Goes, "An Energy-Level Perspective of Bias Temperature Instability," in *Proc. Intl.Rel.Phys.Symp. (IRPS)*, 2008, pp. 28–38.

[15] T. Grasser, H. Reisinger, W. Goes, T. Aichinger, P. Hehenberger, P. Wagner, M. Nelhiebel, J. Franco, and B. Kaczer, "Switching Oxide Traps as the Missing Link between Negative Bias Temperature Instability and Random Telegraph Noise," in *Proc. Intl.Electron Devices Meeting (IEDM)*, 2009, pp. 729–732.

[16] B. Kaczer, T. Grasser, P. Roussel, J. Martin-Martinez, R. O'Connor, B. O'Sullivan, and G. Groeseneken, "Ubiquitous Relaxation in BTI Stressing-New Evaluation and Insights," in *Proc. Intl.Rel.Phys.Symp. (IRPS)*, 2008, pp. 20–27.

[17] T. Aichinger, S. Puchner, M. Nelhiebel, T. Grasser, and H. Hutter, "Impact of Hydrogen on Recoverable and Permanent Damage following Negative Bias Temperature Stress," in *Proc. Intl.Rel.Phys.Symp. (IRPS)*, 2010, pp. 1063–1068.

[18] R. Paulsen and M. White, "Theory and Application of Charge-Pumping for the Characterization of Si-SiO_2 Interface and Near-Interface Oxide Traps," *IEEE Trans.Electron Devices*, vol. 41, no. 7, pp. 1213–1216, 1994.

[19] P. Hehenberger, T. Aichinger, T. Grasser, W. Goes, O. Triebl, B. Kaczer, and M. Nelhiebel, "Do NBTI-Induced Interface States Show Fast Recovery? A Study Using a Corrected On-The-Fly Charge-Pumping Measurement Technique," in *Proc. Intl.Rel.Phys.Symp. (IRPS)*, 2009.

[20] B. Kaczer, V. Arkhipov, R. Degraeve, N. Collaert, G. Groeseneken, and M. Goodwin, "Disorder-Controlled-Kinetics Model for Negative Bias Temperature Instability and its Experimental Verification," in *Proc. Intl.Rel.Phys.Symp. (IRPS)*, 2005, pp. 381–387.

[21] J. Weeks, J. Tully, and L. Kimerling, "Theory of Recombination-Enhanced Defect Reactions in Semiconductors," *Physical Review B*, vol. 12, no. 8, pp. 3286–3292, 1975.

[22] H. Sumi, "Dynamic Defect Reactions Induced by Multiphonon Nonradiative Recombination of Injected Carriers at Deep Levels in Semiconductors," *Physical Review B*, vol. 29, no. 8, pp. 4616–4630, 1984.

[23] A. Lelis and T. Oldham, "Time Dependence of Switching Oxide Traps," *IEEE Transactions on Nuclear Science*, vol. 41, no. 6, pp. 1835–1843, Dec 1994.

[24] J. Conley Jr., P. Lenahan, A. Lelis, and T. Oldham, "Electron Spin Resonance Evidence for the Structure of a Switching Oxide Trap: Long Term Structural Change at Silicon Dangling Bond Sites in SiO_2," *Appl.Phys.Lett.*, vol. 67, no. 15, pp. 2179–2181, 1995.

[25] J. Ryan, P. Lenahan, T. Grasser, and H. Enichlmair, "Recovery-Free Electron Spin Resonance Observations of NBTI Degradation," in *Proc. Intl.Rel.Phys.Symp. (IRPS)*, 2010, pp. 43–49.

[26] M. Alam, "A Critical Examination of the Mechanics of Dynamic NBTI for pMOSFETs," in *Proc. Intl.Electron Devices Meeting (IEDM)*, 2003, pp. 345–348.

[27] T. Grasser, W. Goes, V. Sverdlov, and B. Kaczer, "The Universality of NBTI Relaxation and its Implications for Modeling and Characterization," in *Proc. Intl.Rel.Phys.Symp. (IRPS)*, 2007, pp. 268–280.

[28] L. Tsetseris, X. Zhou, D. Fleetwood, R. Schrimpf, and S. Pantelides, "Physical Mechanisms of Negative-Bias Temperature Instability," *Appl.Phys.Lett.*, vol. 86, no. 14, pp. 1–3, 2005.

[29] S. Volkos, E. Efthymiou, S. Bernardini, I. Hawkins, A. Peaker, and G. Petkos, "The Impact of Negative-Bias-Temperature-Instability on the Carrier Generation Lifetime of Metal-Oxynitride-Silicon Capacitors," *J.Appl.Phys.*, vol. 100, no. 12, pp. 124 103–1–124 103–9, 2006.

[30] D. Brown and N. Saks, "Time Dependence of Radiation-Induced Trap Formation in Metal-Oxide-Semiconductor Devices as a Function of Oxide Thickness and Applied Field," *J.Appl.Phys.*, vol. 70, no. 7, pp. 3734–3747, 1991.

Questions and Answers

Q1: What do you think about waiting long enough to make recoverable portion negligible?

A1: Unfortunately, this is only possible in special circumstances as was shown for a few cases. Normally, when a device is stress under higher stress conditions, recovery will not stop within a week, making this approach unfeasible.

Q2: What are the properties of the metastable neutral state?

A2: The metastable neutral state is characteristic feature of a switching trap: most importantly, it is responsible for the strong bias dependence during recovery as it allows defect annealing via an alternative pathway. The metastable neutral state is also responsible for the temporary RTN (see Grasser et al., IRPS '10)

Q3: What percentage are oxide defects?

A3: Unfortunately, this is hard to say. At the moment it seems to us that most of the degradation is due to oxide defects.higher stress conditions, recovery will not stop within a week, making this approach unfeasible.